Title
3-D Imaging of Crystals at Atomic Resolution

Authors
O'Keefe, M.A.
Downing, K.H.
Wenk, H.R.
et al.

Publication Date
1994

3-D IMAGING OF CRYSTALS AT ATOMIC RESOLUTION

Michael A. O'KEEFE[*], Kenneth H. DOWNING[✧], Hans-Rudolf WENK[❋] and HU Meisheng[❋]

[*]*National Center for Electron Microscopy, UCLBL, Berkeley, CA 94720.*
[✧]*Donner Laboratory, UCLBL, Berkeley, CA 94720.*
[❋]*Department of Geology and Geophysics, University of California, Berkeley, CA 94720.*

Materials Research Society Symposium
on
Determining Nanoscale Physical Properties of Materials by Microscopy and Spectroscopy

Symposium Proceedings **332** (1994) 563-571.
M. Sarikaya, M. Isaacson, H.K. Wickramasinghe (eds.)

Ernest Orlando Lawrence Berkeley National Laboratory – LBNL-35156

3-D IMAGING OF CRYSTALS AT ATOMIC RESOLUTION

Michael A. O'KEEFE[*], *Kenneth H. DOWNING*[✧], *Hans-Rudolf WENK*[❋] *and HU Meisheng*[❋]
[*]*National Center for Electron Microscopy, UCLBL, Berkeley, CA 94720.*
[✧]*Donner Laboratory, UCLBL, Berkeley, CA 94720.*
[❋]*Department of Geology and Geophysics, University of California, Berkeley, CA 94720.*

ABSTRACT

Electron crystallography has now been used to investigate the structures of inorganic materials in three dimensions. As a test of the method, amplitudes and phases of structure factors were obtained experimentally from high resolution images of staurolite taken in a number of different projections. From images in five orientations, a three-dimensional Coulomb potential map was constructed with a resolution of better than 1.4Å. The map clearly resolves all the cations (Al,Si,Fe) in the structure, and all of the oxygen atoms. This method promises great potential for structure determinations of small domains in heterogeneous crystals which are inaccessible to x-ray analysis. Three-dimensional structure determinations should be possible on small domains only approximately 10 unit cells wide, and may resolve site occupancies in addition to atom positions. Given a microscope stage with a suitable range of tilt and enough mechanical stability, the method could also be applied to small crystalline particles larger than about 50Å or 100Å, and to derive the two-dimensional structure of periodic defects.

INTRODUCTION

With recent advances in electron microscope instrumentation, high-resolution electron microscopy has become routine, and point resolutions of better than 2Å have been obtained in images of many inorganic crystals. Although this resolution is sufficient to resolve interatomic spacing, interpretation generally requires comparison of experimental images with calculations [1]. Since the images are two-dimensional representations, or *projections*, of full three-dimensional structures, information in the images is often lost due to overlapping images of atoms at various heights. We have explored the technique of three-dimensional electron crystallography to circumvent this limitation. In three-dimensional electron crystallography, information from several views of a crystal is combined to produce a three-dimensional data set that can provide images of atoms in single atomic layers.

Electron crystallography was originally developed to obtain three-dimensional information on proteins [2,3]. The resolution in images of proteins is severely limited by effects of radiation damage; however, in principle, three-dimensional reconstructions should be obtainable at atomic resolution from specimens that are resistant to damage. The most serious problem would appear to be in obtaining high-resolution images from areas that are thin enough that dynamical scattering effects can be ignored without significant degradation of accuracy, although to some degree dynamical effects can be reduced by slight off-axis tilt of the specimen [4].

To demonstrate the potential of the method for materials, we have used electron crystallography to carry out a determination of the three-dimensional structure of staurolite. The first determination [5] was to a resolution of 1.6Å, produced by using data from images taken at Scherzer defocus in five different directions. A later determination [6] achieved a resolution of 1.4Å by including data from through-focus series of images obtained in each of the five directions previously used. Staurolite, a silicate mineral for which the complex structure is well known [7], is typical of many oxide structures with close-packed oxygen atoms surrounding different cation types in tetrahedral and octahedral coordination; it thus provides a good test of the methodology.

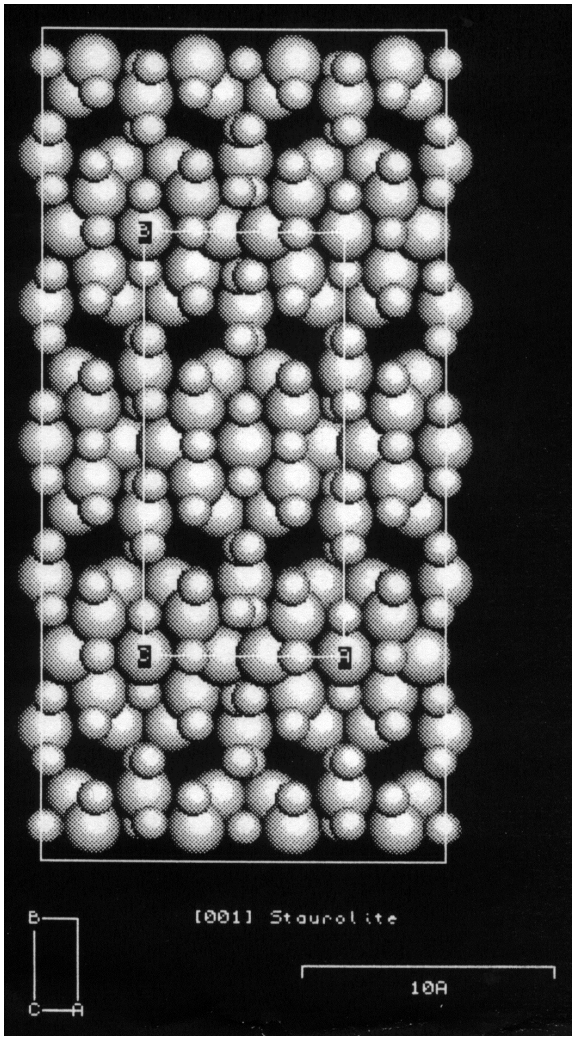

Figure 1 shows the structure of staurolite projected in the [001] direction, displaying the large number of overlapping atoms from the four layers (lying 1.4Å apart along the **c** axis) that make up the unit cell of staurolite. This overlapping of atoms is typical of many materials, including alloys, minerals, and ceramic structures, and leads to difficulty in image interpretation in terms of atomic arrangement. For comparison, figure 2 shows how much more easily the structure can be discerned when the four layers are separated out as individual layers.

In the sections shown in figure 2, all the atoms can be clearly distinguished because no two can be much closer together than the metal-oxygen bond distances. In the xy0 and xy½ sections the distance of closest approach of any two atoms is 1.8Å, whereas in the xy¼ and xy¾ sections, the oxygen atoms lie slightly above and below the z = ¼ and z = ¾ planes, and the projected distance is 1.6Å.

It is obvious that the improvement in the visibility of atoms in sections compared with those in projections will extend to high-resolution electron microscope images. Image simulation can be used to confirm this supposition, and to show just how visible the atoms will be at various

Figure 1. *Projection of the structure of staurolite in the [001] direction. The unit cell (marked) has dimensions* ***a*** *= 7.82Å,* ***b*** *= 16.52Å, and* ***c*** *= 5.63Å.*

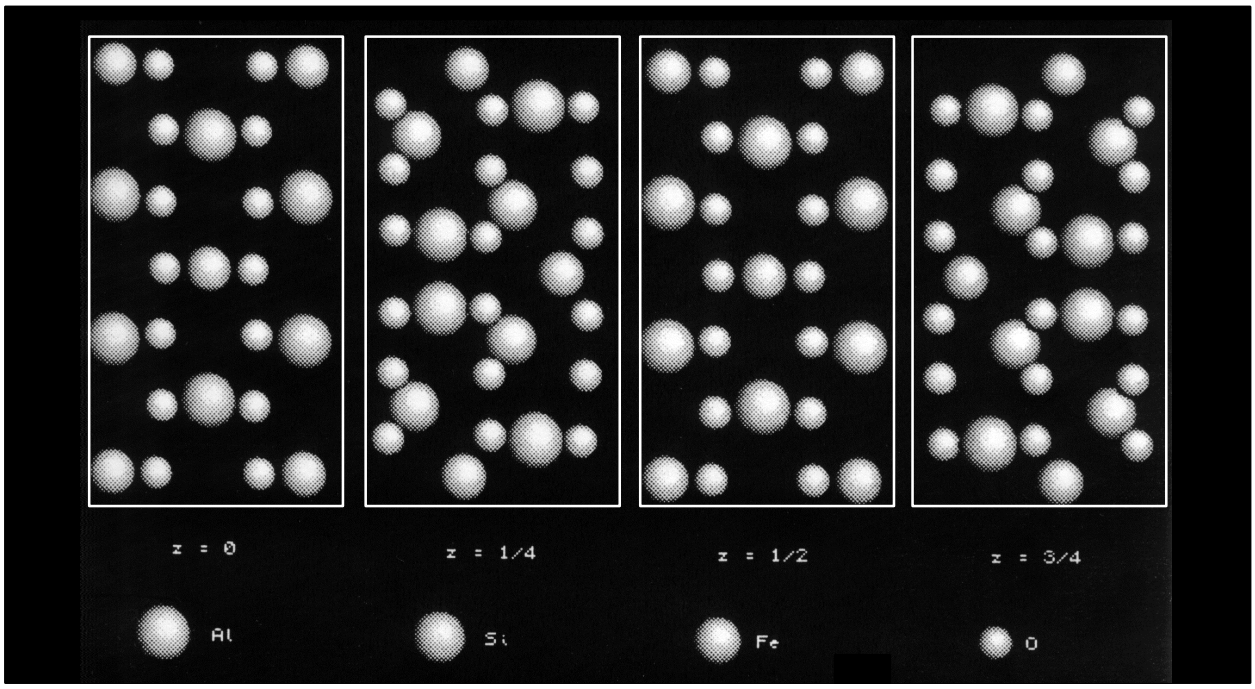

Figure 2*. The four sections making up a unit cell of staurolite. Heights in the [001] direction are z=0, z=¼, z= ½, and z=¾. The z=0 and z=½ are identical, and z=¼ and z=¾ are mirrors.*

electron microscope resolutions. For the thin crystals used in three-dimensional reconstruction, a simple weak-phase-object image formation theory can be used to demonstrate visibility as a function of resolution. Figure 3(a) shows weak-phase-object image simulations for electron microscope images from thin specimens of staurolite viewed in [001] orientation over a range of microscope resolutions. The simulations demonstrate that individual atoms are difficult to discern in images that are a projection of the full unit cell, even at a resolution as good as 1.4Å.

On the other hand, when simulations are computed from just the xy0 and xy¼ sections (fig.3b,c), it is clear that atoms may be distinguished clearly in these sections at 1.6Å resolution (and even at 1.8Å for the xy0 section). Of course, it is not possible to obtain experimental section images directly from the electron microscope, but it is possible to derive approximations to them from a three-dimensional reconstruction derived from projections (images). To form

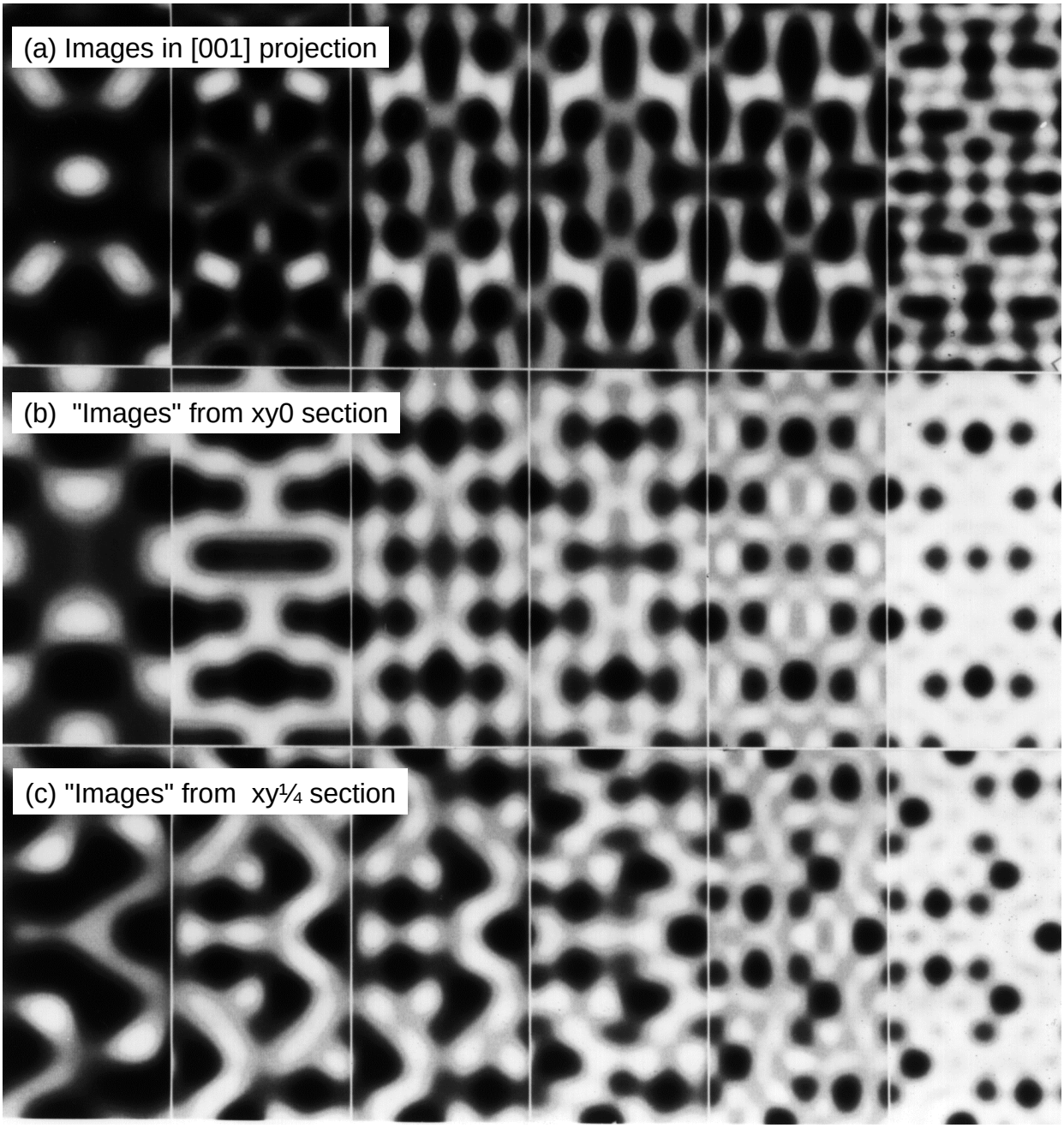

Figure 3*. Weak-phase-object simulations of [001] images of staurolite for the full unit cell (a), the xy0 section (b), and the xy¼ section (c). Resolutions (marked in Å) run from 3.0Å to 1.4Å.*

such a three-dimensional reconstruction requires combining images obtained in several different directions. Figure 4 demonstrates how sets of images are obtained from the three-dimensional specimen over a range of objective lens defocus in each of several directions. The information in the sets of images is then combined to produce a three-dimensional representation of the specimen unit cell.

EXPERIMENTAL

Using the JEOL ARM-1000 at the National Center for Electron Microscopy, we obtained focus series of images at atomic resolution in the three main projections ([100], [010], and [001]). We also used the high angle tilt stage (±40° on two axes) to obtain images perpendicular to [101] and [310]. All the micrographs used for processing came from very thin areas, equivalent to <40Å in the matching simulations (crystal thicknesses derived from matching on-axis simulations to experimental images form a lower limit to experimental specimen thicknesses[4]). In these thin areas, the scattering contribution from the overlying amorphous film is considerable, but the crystalline image component is resolved with sufficient signal-to-noise ratio to enable the structure factors to be extracted reliably. Initially, we selected only micrographs close to Scherzer focus for analysis. Images in the five projections were digitized, and structure factors were extracted from the Fourier transforms, allowing calculation of unit cell projections. Multibeam dynamical scattering image-contrast calculations for the microscope conditions and specimen parameters were computed as a check on the image processing, and agree well with the observed images and the unit cell projections (figure 5). The same is true for diffraction patterns and the optical diffractograms of the images used to extract

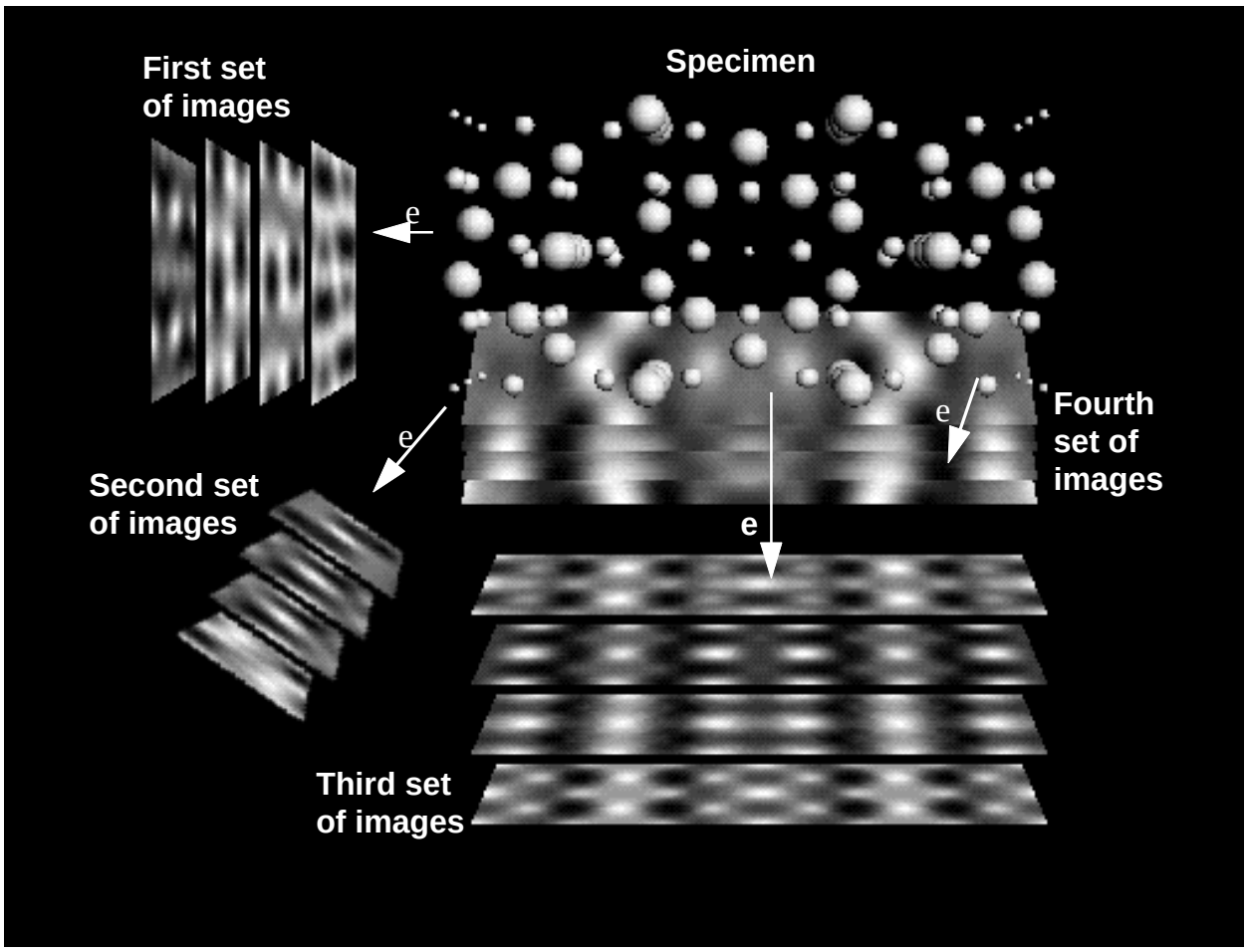

Figure 4. *Illustration of the method of obtaining three-dimensional data in the form of sets of two-dimensional projections (images) of the crystalline specimen.*

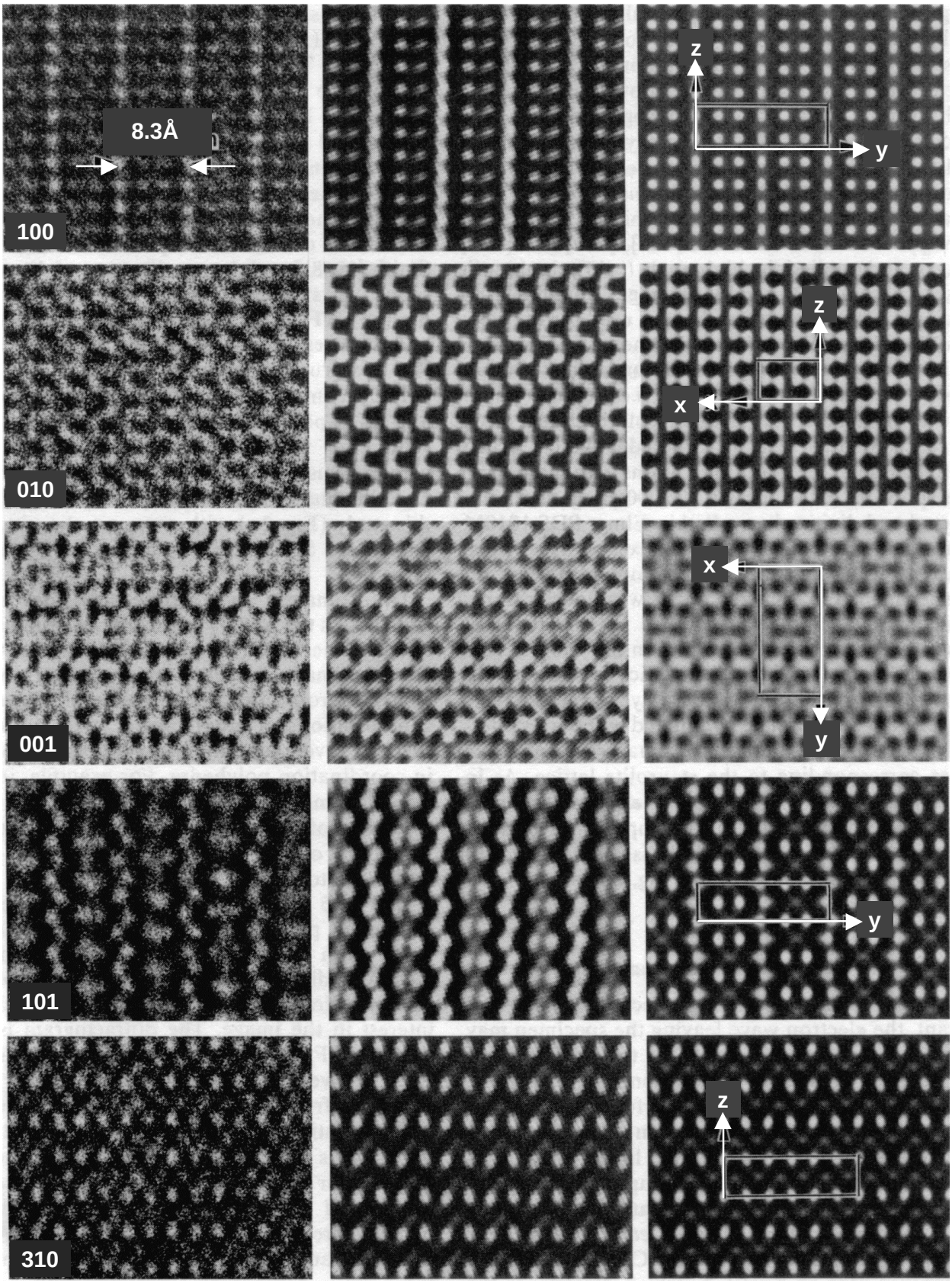

Figure 5. *Scherzer-focus images (left) taken in five directions (marked), processed (center) by Fourier filtering, and compared with simulations (right) for the ARM at 800keV and 50Å crystal thickness.*

experimental structure factors (figure 6). The experimental optical diffractograms show intensity extending to 1.38Å, the value at which the envelope of the contrast transfer function of the JEOL ARM-1000 approaches zero.

In our first determination, we used the five Scherzer-focus images (figure 5) to produce reflections with d >1.6Å because of the uncertainty in determining the sign of the CTF at higher resolution. Symmetry-related reflections within each projection were averaged. Data from the five projections were then combined, using equivalent reflections in different projections for scaling, resulting in measurement of 30 of the 80 unique, non-extinct reflections out to d = 1.6Å. Symmetry operators expanded these 30 structure factors to 72 in half space.

The second structure determination used eight to ten images (in a focal series) from each projection direction, and produced 59 reflections out to 1.38Å, out of 93 possible reflections; these 59 reflections expanded to give 162 structure factors in half space. However, this result did not significantly improve the resolution in the three-dimensional reconstruction because the additional reflections were strongly damped by the actions of the objective lens contrast transfer function (CTF) and the damping functions associated with the effects of partial coherence [8,9].

In the third determination, we included a correction for the fall-off in intensity-spectrum amplitudes due to the objective lens CTF and its damping function [6]; this determination showed improved resolution.

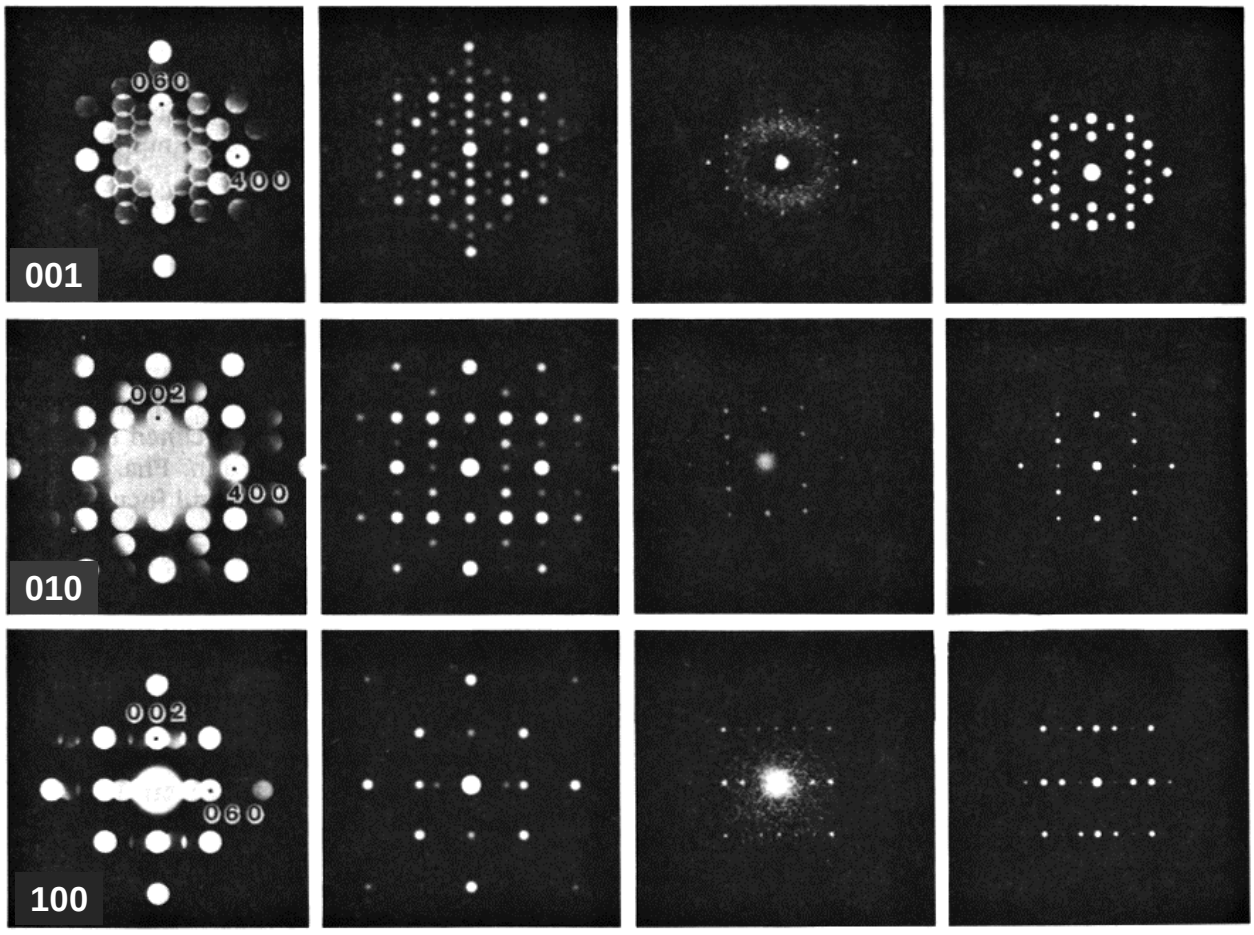

(a) Experimental SAD (b) Simulated SAD (c) Experimental OD (d) Simulated OD

Figure 6. *Diffraction patterns and intensity spectra in the three main directions. (a) experimental selected area diffraction pattern (SAD), (b) simulated SAD, (c) experimental image intensity spectrum (optical diffraction pattern) from image at Scherzer focus, (d) simulated intensity spectrum.*

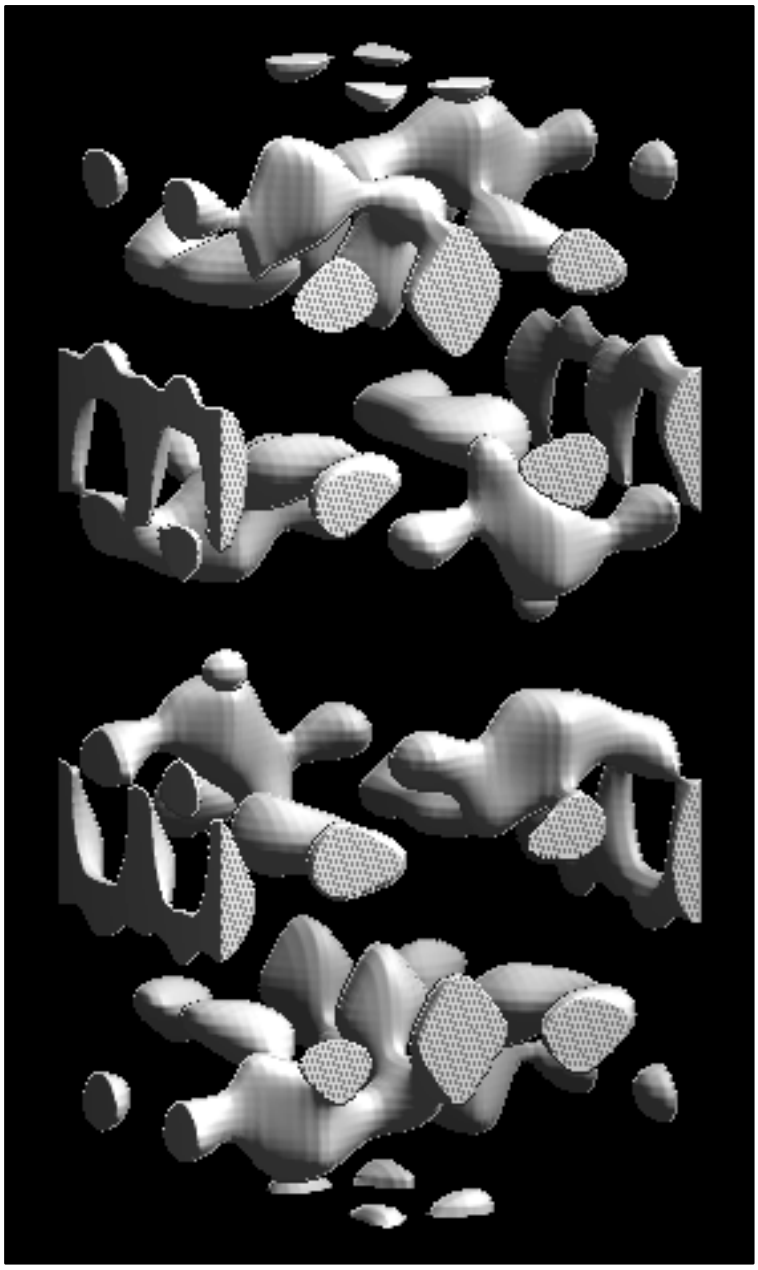

Figure 7*. Surface representation of the three-dimensional Coulomb potential in a full unit cell of staurolite, at a density level that displays all fully occupied cations and oxygens; the view is close to [001].*

Because the five projections of staurolite that we used were centrosymmetric, structure factor phases were either 0° or 180°. The phases were determined directly from the Fourier transform of the image (image intensity spectrum) after shifting to the proper phase origin[2]. Amplitudes could be obtained either directly from electron diffraction patterns or from the transform of the image. We have used the latter. Because electron diffraction patterns average over large areas of varying thickness, it is advantageous to obtain amplitude information from images, even though they are affected by the contrast transfer function. Image simulations for staurolite show that dynamical effects should not be significant in our data. Amplitudes vary linearly with thickness up to an on-axis simulation thickness of 50Å; above that, changes become irregular due to dynamic scattering. In the centrosymmetric case, phases derived from the images are less affected by dynamical effects, and are reliable for thickness up to 100Å.

RESULTS

The three-dimensional potential map calculated from our third determination of the experimental structure factors is illustrated in figure 7 as a three-dimensional surface enclosing all of the cations and associated oxygen atoms that are present at full occupancy.

Since all atoms are located near planes equivalent to z = 0 and z = ¼, and because of the assumed orthorhombic symmetry, most of the information is contained in these two xy sections. Figure 8 compares the experimental results obtained from the three determinations, displayed in the [001] direction, both as projections of the unit cell, and as xy sections. There is excellent correspondence between the experimental results and the weak-phase object (WPO) simulations of figure 3. While the second determination (at a nominal resolution of 1.38Å) shows a slight improvement over the first (at 1.6Å), most improvement occurs in the third determination, in which CTF correction was included. The results of the third determination match the 1.4Å WPO simulation for the full unit cell projection, and clearly resolve all atom positions in the xy sections. Note that the partially occupied octahedral Al site at 1/2 1/2 0 has a much lower potential than the fully occupied sites (e.g., 1/2 1/6 0).

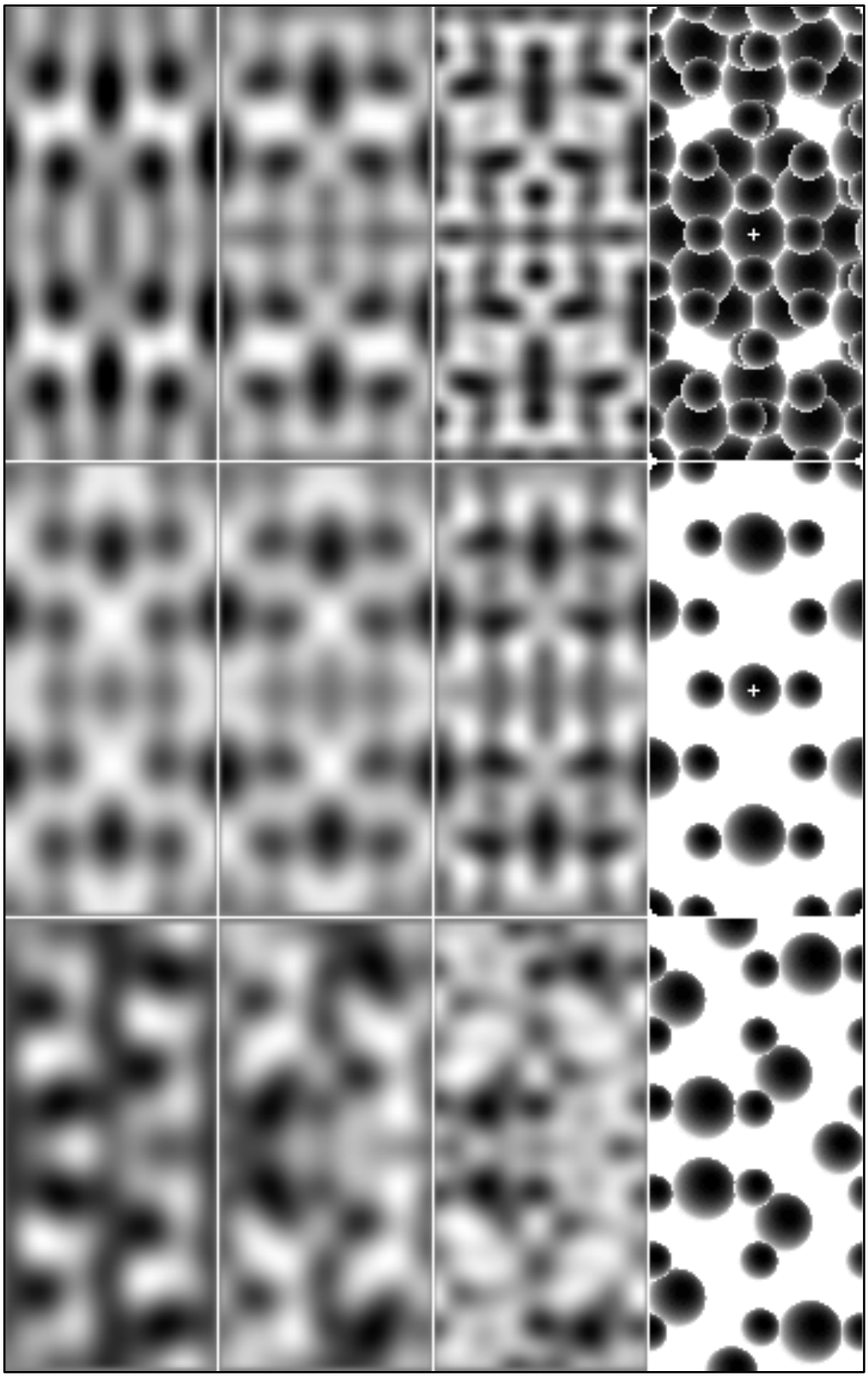

Figure 8. *Projections (upper), and sections at z=0 (center) and z=¼ (lower) from the three experimental determinations. The first column shows results from the determination from 30 reflections to 1.6Å, the second from 59 reflections to 1.38Å, and the third includes CTF correction. Note the correspondence of the 1.38Å projection to the 1.4Å WPO image from the model (top right in figure 3). The fourth column shows the model for comparison.*

DISCUSSION

We have demonstrated the procedure of three-dimensional reconstruction for staurolite in order to show the steps required. It is clear that three-dimensional reconstruction can enable us to construct images which resolve atoms that are normally overlapped in any one electron microscope image, including lighter atoms such as oxygen in the presence of heavier metal atoms; the fact that individual atoms in a close-packed structure, including the oxygen atoms, can be separated is attributed to the three-dimensional reconstruction. The technique has obvious application to the oxide-superconductor structures.

In addition, once the process of image processing is routinely applied, it becomes simple to extend the microscope resolution by reconstruction from a focal series; in our third structure determination (even before applying any three-dimensional reconstruction) CTF correction and reconstruction from focal series produced images from the ARM-1000 with a full 1.4Å resolution instead of the routine 1.6Å available at Scherzer defocus. Such resolution-extension will become of much greater importance as high-resolution electron microscopes equipped with field-emission guns become more prolific.

CONCLUSIONS

We see great potential for three-dimensional electron crystallography in determination of unknown crystal structures, particularly where homogeneous regions exist only in submicrometre-sized domains. Such heterogeneous crystals have been increasingly recognized in metals, ceramics and minerals. We estimate that a three-dimensional structure determination should be possible on areas only about 10 unit cells across, provided only that a sufficient number of projections can be recorded. In addition, where defects are periodic, the technique should be applicable to the supercell created by the periodic defects. Our own efforts are proceeding into applying three-dimensional reconstruction to the case of periodic defects such as grain boundaries in metals and periodic oxygen vacancies in superconductors.

ACKNOWLEDGMENTS

The authors wish to thank J.H. Turner for assistance with the figures and David J. Smith with the text. NCEM facilities are available to qualified microscopists at no cost; they and this work are supported by the Director, Office of Energy Research, Office of Basic Energy Sciences, Materials Science Division of the U.S. Department of Energy under contract no. DE-AC03-76SF00098. In addition, KHD is supported in part by NIH grant GM 36884. Support from the National Science Foundation (EAR88 16577 to HRW), the University of California Education Abroad Program (to HM and HRW) is also gratefully acknowledged.

REFERENCES

1. M. A. O'Keefe, P. R. Buseck, & S. Iijima, Nature **274**, 322-324 (1978).
2. L. A. Amos, R. Henderson, & P. N. T. Unwin, Prog. Biophys. Molec. Biol. **39**, 183 (1982).
3. R. M. Glaeser, Ann. Rev. Phys. Chem. **36**, 243-275 (1985).
4. M.A. O'Keefe and V. Radmilovic, in 51st Ann Proc. MSA, Cinc., Ohio, 980-981 (1993).
5. K. H. Downing, Hu Meisheng, H.-R. Wenk & M. A. O'Keefe, Nature **348**, 525 (1990).
6. H-R. Wenk, K.H. Downing, Hu Meisheng & M.A. O'Keefe, Acta Cryst. A**48**, 700 (1992).
7. J. V. Smith, Amer. Mineral. **53**, 1139-1155 (1968).
8. M.A. O'Keefe, in 37th Ann. Proc. EMSA, San Antonio, Texas, 556-557 (1979).
9. M.A. O'Keefe, Ultramicroscopy **47**, 282-297 (1992).